Jakub KOŁOTA, Sławomir STĘPIEŃ

Poznań University of Technology, Chair of Computer Engineering

Analysis of 2D and 3D Finite Element Approach of a Switched Reluctance Motor

Streszczenie. *W pracy zaprezentowano metodę modelowania i symulacji numerycznej silnika reluktancyjnego w ujęciu 2D i 3D, wykorzystując metodę elementów skończonych. W proponowanym modelu, równania pola elektromagnetycznego, oraz równania obwodu elektrycznego są ściśle sprzężone i rozwiązywane wraz z równaniem ruchu w każdym kroku czasowym. Zaprezentowano porównanie dynamiki silnika za pomocą wyników symulacji 2D i 3D oraz omówiono zależności pomiędzy modelami (**Analiza przybliżeń 2D i 3D w metodzie elementów skończonych silnika SRM**).*

Abstract*. A method of modeling and numerical simulation of a switched reluctance motor employing 2D and 3D finite element models is presented. In proposed model, the electromagnetic field equations and the circuit equations are strongly coupled and solved together with motion equation at each time step. The comparison of the motor dynamics using 2D and 3D approach is given considering the relation between different modeling technique.*

Słowa kluczowe: silnik reluktancyjny, metoda elementów skończonych, modelowanie 2D i 3D.
Keywords: switched reluctance motor, finite element method, 2D and 3D modeling technique.

Introduction

Modeling and simulation is preferred method in designing motors compared to building motor prototypes which is more costly. A powerful method, in recent years, is the finite element method used to compute dynamic and steady state conditions of the machine.

Many papers present 2D models, where the electromagnetic field models are coupled with the electric circuit and motion equations. However, the 2D models do not provide enough information, because assume the zero axial flux. This is the basis of the 2D approach [4,6,8-10].

The 3D analysis makes possibility to model the full geometry of the device. In case of the electric circuit approximation, the end-coil effect may be considered. It has an impact on the circuit parameters such a self or mutual inductance. Then, the current response, torque, motion may have quite different waveforms than in the 2D approach [3,5,7,11,17].

The problem of the modeling accuracy is specially visible determining the switching excitation for brushless motors such switched reluctance motors. The switching states are the function of the rotor position, hence determination of the exact control signal requires an exact and precise modeling [3,4,5,9,12-15].

In this paper, a method of modeling and numerical simulation of a variable reluctance stepper motor employing 2D and 3D finite element models is presented. The intention of this paper is to show the impact on the motor dynamics, when the end-coil effect is neglected or considered. Numerical results present the current response, torque and motor speed in both cases.

Model of the VR stepper motor

In the time-stepping finite element technique, the inputs are stator phase voltages, motor geometry and material characteristics, whereas all the other variables such as magnetic vector potentials, currents, the rotor position are calculated.

The use of the 3D finite element method to analyze differences in the current response, the torque and position response of the motor considering 2D model and an existence of the end-coil effect in the 3D approach is described in this article. Figure 1 shows the configuration of the motor and Table 1 presents its main physical parameters.

The motor field model is represented by magnetic vector potential. The equations that describe the magnetic field is written in the cylindrical co-ordinate system. In the area of the stator conductor the field equation may be represented as

$$\nabla \times \left(\frac{1}{\mu} \nabla \times \mathbf{A} \right) - \mathbf{j} = 0 \cdot \tag{1}$$

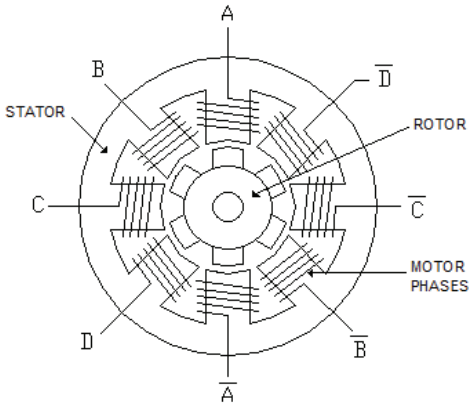

Fig. 1. Reluctance stepper motor configuration

Table 1. The main parameters of the motor

Quantity	Value	Unit
Outer diameter of stator	39	mm
Inner diameter of stator	34	mm
Outer diameter of rotor	26,96	mm
Inner diameter of rotor	18	mm
Air gap width	0,02	mm
Motor length	30	mm
Resistance/phase	15	Ω
Rotor inertia	8,5	gcm^2
Friction	10^{-5}	Nms

The magnetic vector potential **A** is the magnetic field variable, μ is a permeability, **j** is a current density of the thin winding. In this model the eddy current problem is ignored, because the stator and rotor are laminated and the iron losses has a very small impact on the motor dynamics in this case [3,17].

The stator phase circuit equation for the described stepper motor is

$$\frac{d}{dt} \oint_{l_s} \mathbf{A} \mathbf{dl} = u_s - R i_s \,, \tag{2}$$

where s={1,..,4} denotes the phase number, R is a winding resistance of a one phase, i is a phase current and u is a supply voltage.

In the prescribed speed case, the rotor displacement is evaluated by solution of the equation defined as follows:

(3) $$J\frac{d^2\Theta}{dt^2}+b\frac{d\Theta}{dt}=T\,,$$

where Θ is the rotor displacement, , J is the rotor inertia, b is the damping coefficient, $T=T_E-T_L$ is the difference between the electromagnetic and the load torque.

From the approach (1) is derived the matrix equations system, where the weighting functions are the same as the shape functions. The solution of the equation (1) is obtained by minimizing the corresponding energy functional. The minimization is performed by means of the finite element method using 27-node, first order cylindrical elements. The magnetic vector potential may be expressed by

(4) $$\mathbf{A}=\sum_{i=1}^{27}N_i\mathbf{A}_i$$

where N_i are the element shape functions and the $\mathbf{A}_i$ are the approximations to the vector potentials at the nodes of the elements. Introducing the finite element method with the boundary value problem (1) and coupling to the electric circuit model (2), the following system of equations is obtained in the magnetic field [6,17]:

(5) $$\begin{bmatrix}\mathbf{C} & \mathbf{E}\\ \dfrac{\mathbf{F}}{\Delta t} & \mathbf{R}\end{bmatrix}\begin{bmatrix}\mathbf{A}^{t+\Delta t}\\ \mathbf{I}^{t+\Delta t}\end{bmatrix}=\begin{bmatrix}\mathbf{0}\\ \mathbf{U}^{t+\Delta t}+\dfrac{\mathbf{F}}{\Delta t}\mathbf{A}^{t}\end{bmatrix}$$

where: **A** - represents the vector of the unknown vector potentials, **I** - represents the vector of the unknown phase currents, **C** - represents the symmetrical matrix related to the magnetic field, **R** - represents the diagonal matrix related to the winding resistances, **E** - represents the matrix related to the winding currents and the permanent magnets magnetization, **F** - represents the matrix related to the linkage flux, **U** - represents the vector corresponding to the voltage control.

The presented system of the field equations (5) is nonsymmetrical and solved at each iteration step by the preconditioned bi-conjugate gradient algorithm (BiCG) dedicated for the large and sparse linear systems.

The discrete equation of motion is derived from the form of (3). The discrete rotor speed ω and displacement Θ are determined using the backward Euler's approximation for the motion equation.

(6) $$\begin{bmatrix}1 & -\Delta t\\ 0 & 1+\Delta t\dfrac{b}{J}\end{bmatrix}\begin{bmatrix}\Theta^{t+\Delta t}\\ \omega^{t+\Delta t}\end{bmatrix}=\begin{bmatrix}\Theta^{t}\\ \omega^{t}+\Delta t\dfrac{1}{J}T^{t+\Delta t}\end{bmatrix}$$

The motion in the electromagnetic field is realized using the fixed grid technique. The grid of discretisation is independent of the rotor position. The moving body displacement is updating at each iteration step. This approach enables to overcome the stability loss during the solution of the field equations (5). The field model (5) and the motion model (5) are coupled and solved at each iteration step.

At each time step, the global torque is calculated using the Maxwell stress method and eggshell approach [1,2,9,15,16]. The force is evaluated along a surface in the air-gap around the rotor. The torque is obtained from the relationship:

(7) $$\mathbf{T}=\oint_S\{\mathbf{r}\times\mathbf{P}\}\mathbf{dS}\,,$$

where **r** is the position vector of the integration contour, **P** denotes the stress component defined around the rotor, **dS** is a surface segment [17]. Only z-component of the torque $\mathbf{T}=\begin{bmatrix}0 & 0 & T\end{bmatrix}^T$ is taken into consideration.

Experiment

The numerical technique described in this paper is applied to obtain the current waveforms, speed and torque characteristics of the switched reluctance motor excited by square wave signal with amplitude 30V. The device consist of four-phase windings with eight slots (108 turns each).

In the numerical experiment, proposed numerical model is applied to investigate end-coil impact on electromechanical characteristics of the motor. The problem is examined using the 3D first order approach, in which the eddy current problem is neglected and the motor is free of the load torque.

There are considered two situation: modeling a 2D approach using 3D tool neglecting end-coil effect and full 3D modeling considering the end-coil effect. In the assumed approach, a half of the full length has been analyzed and each mesh includes: the rotor discretisation and the stator discretisation including the thin coil system and the airgap. The motor meshes are shown in Figure 2 and Figure 3.

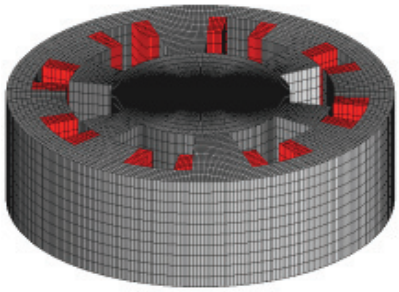

Fig. 2. The 2D approach – the mesh free of end-coils

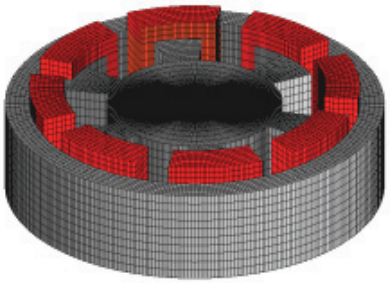

Fig. 3. Full 3D mesh of the motor

The 3D simulation focuses on the end region of the switched reluctance motor model. In the developed problem, the suitable uniform discretisation of the end-coil region and its surrounding air region is very important.

The model is free of the eddy current and magnetic nonlinearity i.e. the B-H relationship is assumed to be linear. To show the difference between obtained results for both approaches, the current response, the torque and the rotor speed is presented.

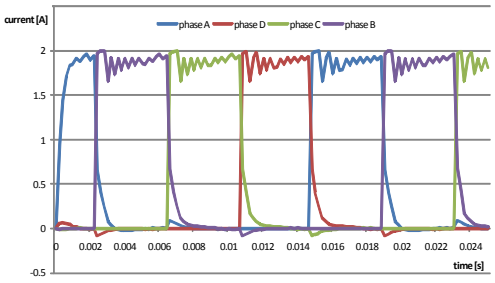

Fig. 4. Transient of the phase currents using 2D model

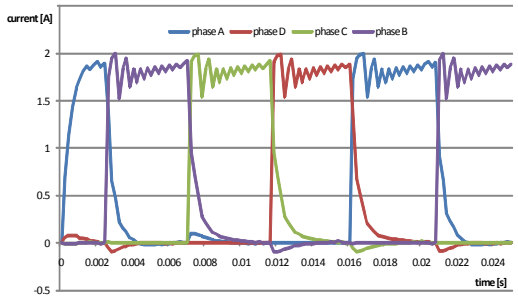

Fig. 5. Transient of the phase currents using 3D model

Figure 4 and 5 show phase currents in the motor. When compare the time of the rising edge of the current in the 3D case due to the 2D during the phase switching state, it is visible that the time constant of each circuit is greater.

To try to clarify the situation, the 3D model includes additional region at the end of the stator where an additional non-zero flux is generated. The stator windings are not

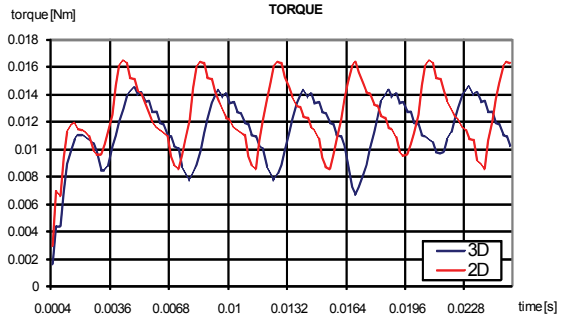

Fig. 6. Torque waveform obtained for 2D and 3D models

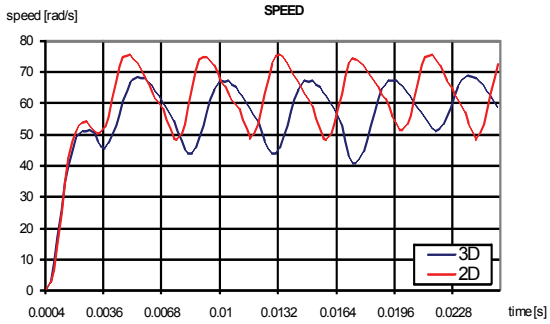

Fig. 7. Comparison of the speed using 2D and 3D approach

As shown in Figure 6 and Figure 7, the effect of an exact modeling of the electric circuit also influences on the torque and speed waveforms. The predicted torque for the 3D case, seems to be delayed with decreased peak. It is an effect of the current course because the torque is the nonlinear function of the current. Moreover, the torque is computed employing greater integration surface enlarged by the air region related to the end-coils extra discretisation. It also results in the computed rotor speed. The speed is more smooth and somewhat lower.

Conclusions

All of the above research reflect a fact that in spite of the weak magnetic field in the end region, the magnetic field is complicated in the spatial distribution, so the magnetic force density fluctuates in the end-coil. The 3D simulation enlarge time constant coefficient, so the main dynamic characteristics of the motor are more gentle. The difference occurs, especially when the axial length of the machine is relatively short. The 2D model of variable stepper motor neglects all axial flux paths, that especially exists in the air-gap and can only be used to analyze certain aspects like detent torque or holding torque around small stationary working points.

More systematic analysis for the effects of the permeability and the conductivity of the pole piece, and the frequency of the power source on the difference of the flux and eddy current distributions between 2D and 3D analyses will be reported in future work. The effects of the nonlinearity of the pole piece should also be examined.

REFERENCES

[1] Henrotte F., Deliége G., Hameyer K., The eggshell approach for the computation of electromagnetic forces in 2D and 3D, *COMPEL*, Vol. 23 (2004), No. 4, 996-1005

[2] Henrotte F., Handbook for the computation of electromagnetic forces in a continuos media, *ICS Newsletter*, Vol. 11(2004), No. 2, 10-17

[3] Ranran L., Arkkio A., A 3-D magnetostatic analysis and calculation of parameters in end region of an induction machine, *Transmission and Distribution Conference and Exposition*, No.1109/TDC.2008.4517190, 1-6

[4] Oliveira A. De, Antunes R., Kuo-Peng P., Sadowski N. and Dular P., Electrical machine analysis considering field – circuit – movement and skewing effects, *COMPEL*, Vol. 23 (2004), 1080-1091

[5] Fu W. N., Ho S. L., Enhanced nonlinear algorithm for the transient analysis of magnetic field and electric circuit coupled problems, *IEEE Trans. Magn*. Vol. 45 (2009), 701–706

[6] Bernat J., Kołota J.,Stępień S., Coupled field-motion model of variable reluctance stepper motor, *Electrical Review*, Vol.4 (2009), 210-213

[7] Krishnan R., Switched Reluctance Motor Drives. Modeling, Simulation, Analysis, Design, and Applications (ser. I. E.. Boca Raton, FL: CRC Press, 2001)

[8] Roux C., Morcos M. M., On the use of a simplified model for switched reluctance motors, *IEEE Trans. Energy Conv*. Vol. 17 (2002), 400–405

[9] Vijayakumar K., Karthikeyan R., Paramasivam S., Arumugam R., and Srinivas K., Switched Reluctance Motor Modeling, Design, Simulation, and Analysis: A Comprehensive Review, *IEEE Trans. Mag*., Vol. 44 (2008), 4605-4617

[10] Arumugam R., Lowther D., Krishnan R. and Lindsay J., Magnetic field analysis of a switched reluctance motor using a two dimensional finite element model, *IEEE Trans. Magn*. Vol. 21 (1985), 1883–1885

[11] Harris M. R. and Sykulski J. K., Simple method for calculating the peak torque of a switched reluctance motor: a computational investigation, *COMPEL*, Vol. 11 (1992),193-196

[12] Finch J., Metwally H., Harris M. R., Switched reluctance motor excitation current: Scope for improvement, in Proc. *IEE Power Electronics and Variable-Speed Drives Conf*. (1986) 196–199.

[13] Mao S. H., Tsai M. C., An analysis of the optimum operating point for a switched reluctance motor, *J. Magn. Magn. Mater*. Vol. 282 (2004), 53–56

[14] Wu W., Dunlop J., Stephen B., Collocott J. and Kalan B., Design optimization of a switched reluctance motor by electromagnetic and thermal finite-element analysis, *IEEE Trans. Magn.* Vol. 39 (2003), 3334–3336

[15] Rahman K. M. and Schulz S. E., Design of high-efficiency and high torque density switched reluctance motor for vehicle propulsion, *IEEE Trans. Ind. Appl.*, Vol. 38 (2002), 1500–1507

[16] Stępień S., Determination of electromagnetic torque with on-line computation of the optimal radius of the integration contour, *COMPEL* Vol. 29 (2010), 686-698

[17] Stępień S., Bernat J., Modeling and optimal control of variable reluctance stepper motor, *COMPEL*, Vol. 30 (2011), 726-740

***Autorzy**: dr inż. Sławomir Stępień, Poznan University of Technology, Chair of Computer Engineering, ul. Piotrowo 3a, 60-965 Poznan, E-mail:* Slawomir.Stepien@put.poznan.pl*;*
dr inż. Jakub Kołota, , Poznan University of Technology, Chair of Computer Engineering, ul. Piotrowo 3a, 60-965 Poznan, E-mail: Jakub.Kolota@put.poznan.pl*;*